

## Subcellular Localization of the $\alpha$ and $\beta$ Subunits of the Acute Myeloid Leukemia-Linked Transcription Factor PEBP2/CBF

JIE LU,<sup>1</sup> MITSUO MARUYAMA,<sup>1</sup> MASANOBU SATAKE,<sup>1†</sup> SUK-CHUL BAE,<sup>1</sup> EIKO OGAWA,<sup>1</sup>  
HIROSHI KAGOSHIMA,<sup>2</sup> KATSUYA SHIGESADA,<sup>2</sup> AND YOSHIAKI ITO<sup>1\*</sup>

*Departments of Viral Oncology<sup>1</sup> and Genetics and Molecular Biology,<sup>2</sup> Institute for  
Virus Research, Kyoto University, Sakyo-ku, Kyoto 606, Japan*

Received 11 August 1994/Returned for modification 23 September 1994/Accepted 9 December 1994

**Each of the two human genes encoding the  $\alpha$  and  $\beta$  subunits of a heterodimeric transcription factor, PEBP2, has been found at the breakpoints of two characteristic chromosome translocations associated with acute myeloid leukemia, suggesting that they are candidate proto-oncogenes. Polyclonal antibodies against the  $\alpha$  and  $\beta$  subunits of PEBP2 were raised in rabbits and hamsters. Immunofluorescence labeling of NIH 3T3 cells transfected with PEBP2 $\alpha$  and  $\beta$  cDNAs revealed that the full-size  $\alpha$ A1 and  $\alpha$ B1 proteins, the products of two related but distinct genes, are located in the nucleus, while the  $\beta$  subunit is localized to the cytoplasm. Deletion analysis demonstrated that there are two regions in  $\alpha$ A1 responsible for nuclear accumulation of the protein: one mapped in the region between amino acids 221 and 513, and the other mapped in the Runt domain (amino acids 94 to 221) harboring the DNA-binding and the heterodimerizing activities. When the full-size  $\alpha$ A1 and  $\beta$  proteins are coexpressed in a single cell, the former is present in the nucleus and the latter still remains in the cytoplasm. However, the N- or C-terminally truncated  $\alpha$ A1 proteins devoid of the region upstream or downstream of the Runt domain colocalized with the  $\beta$  protein in the nucleus. In these cases, the  $\beta$  protein appeared to be translocated into the nucleus passively by binding to  $\alpha$ A1. The chimeric protein containing the  $\beta$  protein at the N-terminal region generated as a result of the inversion of chromosome 16 colocalized with  $\alpha$ A1 to the nucleus more readily than the normal  $\beta$  protein. The implications of these results in relation to leukemogenesis are discussed.**

A murine transcription factor, PEBP2, was originally identified as a polyomavirus enhancer core-binding protein (15, 42) interacting with the region termed the PEA2 site (37). The polyomavirus enhancer is nonfunctional in embryonal carcinoma F9 cells and becomes functional after the cells are induced to differentiate into endoderm-like cells (10, 18, 44). PEBP2 is undetectable in the former state (1, 20) but becomes detectable in the latter state of F9 cells (1). Therefore, PEBP2 is partly responsible for such properties of the polyomavirus enhancer. PEBP2 is composed of two structurally unrelated subunits,  $\alpha$  and  $\beta$  (33, 35). The  $\alpha$  subunit contains a 128-amino-acid (aa) region highly homologous to the corresponding region of the product of a *Drosophila* segmentation gene, *runt* (35). This evolutionarily conserved region is termed the Runt domain and encompasses the DNA-binding and dimerization domains (13). The high degree of homology to the Runt protein supports the view that PEBP2 is likely to be a factor involved in the early mammalian embryo development. A transcription factor, CBF, originally identified as the murine leukemia virus enhancer core-binding protein, has been found to be identical to PEBP2 (46).

Another member of the Runt domain coding genes, human *AML1*, was identified at the breakpoint of the 8;21 chromosome translocation, a characteristic chromosomal abnormality associated with a major subtype of acute myeloid leukemia (28). As a result of t(8;21), a chimeric protein, *AML1/MTG8* (ETO), which is composed of the amino-terminal portion of

the *AML1* protein including the Runt domain fused to a zinc finger-containing polypeptide encoded in chromosome 8 is produced (8, 19, 27, 30, 32). *AML1/MTG8* (ETO) has, therefore, a potential to bind to the PEBP2 site and form a dimer with the  $\beta$  protein. This chimeric protein is believed to be responsible for leukemogenesis (40). *AML1* has also been detected at the breakpoints of t(3;21) myeloid leukemia (25). Involvement of PEBP2 in human leukemia was further strengthened by a recent discovery that the gene encoding the human homolog of the  $\beta$  subunit is located at the breakpoint of inversion 16, characteristic of another subtype of acute myeloid leukemia. The chimeric protein, PEBP2 $\beta$ /CBF $\beta$ -MYH11, produced as a result of *inv*(16) contains a large part of the  $\beta$  protein at the amino-terminal region fused to the carboxy-terminal region of the smooth muscle myosin heavy chain (22). The portion of the  $\beta$  protein in the chimeric protein is sufficient to form a dimer with the  $\alpha$  protein (33). Abnormalities of either the  $\alpha$  or the  $\beta$  subunit, therefore, appear to cause the same type of leukemia.

Three distinct genes, *PEBP2 $\alpha$ A* (35), *PEBP2 $\alpha$ B* (2, 4), and *PEBP2 $\alpha$ C* (3), which encode the mammalian Runt domain proteins have been detected. *PEBP2 $\alpha$ B* is the mouse homolog of human *AML1* (2, 4). The  $\alpha$  subunit binds to DNA weakly, while the  $\beta$  subunit binds to the  $\alpha$  protein and increases its affinity for DNA without interacting with DNA by itself (33, 35). Expression of *PEBP2 $\alpha$ A* and *PEBP2 $\alpha$ B* is highly tissue specific (4, 35); most notably, both are expressed in T cells throughout the development of thymus (43). Expression in established cell lines suggests that *PEBP2 $\alpha$ A* appears to be T cell specific (35), while *PEBP2 $\alpha$ B* is expressed in pre-B cells in addition to T cells (4). *AML1/ $\alpha$ B* is also expressed in human myeloid leukemia-derived cell lines (25, 28, 40). On the con-

\* Corresponding author. Phone: 81-75-751-4028. Fax: 81-75-752-3232.

† Present address: Department of Molecular Immunology, Institute of Development, Aging and Cancer, Tohoku University, Seiryomachi 4-1, Aoba-ku, Sendai 980, Japan.

trary, expression of *PEBP2 $\alpha$ C* and the  $\beta$  subunit gene is ubiquitous (3, 33, 46). The *Drosophila* Runt protein is a nuclear protein (17). Mammalian Runt domain-containing proteins are DNA-binding proteins. Therefore, it is expected that the mammalian Runt domain proteins are also nuclear proteins. On the other hand, no clue to the subcellular localization of the  $\beta$  protein that has no DNA-binding activity by itself yet acts as a transcription factor by associating with the DNA-binding partner protein has been available.

In the present study, we raised polyclonal antisera against the  $\alpha$  and  $\beta$  subunits and examined their subcellular localizations. The  $\alpha$  protein was found to be localized to the nucleus as predicted, while the  $\beta$  protein was a cytoplasmic protein. The results obtained in the present study suggested that the intracellular dynamic movement of these proteins is one important facet of the regulatory process of *PEBP2* site-dependent transcriptional regulation.

## MATERIALS AND METHODS

**Cell culture and DNA transfection.** NIH 3T3, Ha-*ras*-transformed NIH 3T3, and COS-7 cells were maintained in Dulbecco modified Eagle medium supplemented with 10% (vol/vol) calf serum (former two cell lines) and fetal bovine serum (COS-7). DNA transfection was performed by a calcium phosphate coprecipitation procedure, as modified by Chen and Okayama (6). All transfection experiments were performed with 20  $\mu$ g of plasmid DNA per 10-cm-diameter dish. All transfection experiments were repeated at least twice.

**Construction of plasmids.** The bacterial expression plasmids pET $\alpha$ A1 and pET $\beta$ 2, which harbor the entire coding regions of *PEBP2 $\alpha$ A1* and *PEBP2 $\beta$ 2*, respectively, were described previously (33, 35). pET $\alpha$ A1C17 carries the C-terminal 17-kDa region (aa 359 through 513) of the  $\alpha$ A1 coding sequence. An oligonucleotide, 5'-TATGGCCGGCGTTCAGAACTGGGCC-3', containing the initiation codon ATG was inserted into pET $\alpha$ A1 at the site from which a 1.1-kb *ApaI-NdeI* fragment carrying the N terminus of  $\alpha$ A1 had been removed. pQE9- $\alpha$ A1 contains the entire coding sequence of  $\alpha$ A1 tagged with a histidine cluster at the N terminus, which was generated by swapping the C-terminal region of  $\alpha$ A2 in pQE9- $\alpha$ A2 (35) with that of  $\alpha$ A1 in pET $\alpha$ A1 through use of a *HindIII-PstI* fragment.

For expression vectors in mammalian cells, the *XbaI* fragments from pCDMP $\alpha$ A1, pCDMP $\alpha$ A2[ $\alpha$ A1(1-306)], and pCDMP $\beta$ 1 (35) were cloned into the *XbaI* site of pEF-BOS (29) lacking the simian virus 40 *ori* sequence (16), resulting in pEF- $\alpha$ A1, pEF- $\alpha$ A2[ $\alpha$ A1(1-306)], and pEF- $\beta$ 1, respectively. pEF- $\beta$ 2 and pEF- $\beta$ 3 were similarly constructed. The blunt-ended *BamHI-PvuII* fragments from pQEN93C306, pQEN1C226, and pQEN1C158 (35) were then inserted into the blunt-ended *XbaI* site of pEF-BOS to make pEF- $\alpha$ A1(94-306), pEF- $\alpha$ A1(1-226), and pEF- $\alpha$ A1(1-158). pEF- $\alpha$ B1 and pEF- $\alpha$ B2 were described previously (2). pEF- $\alpha$ A1(1-94) was constructed by inserting a translation terminator linker, 5'-CATGTGAATTCGGAT-3', into the *NcoI* site of pEF- $\alpha$ A1. A 6.2-kb *HindIII* fragment from pEF- $\alpha$ A1 harboring the C-terminal half of  $\alpha$ A1 was replaced with a 1.6-kb *HindIII* fragment from pEF- $\alpha$ A1(94-306) to construct pEF- $\alpha$ A1(94-513). pEF- $\alpha$ B1(1-446) lacking 5 aa at the C-terminal end of  $\alpha$ B1 was made with a Transformer site-directed mutagenesis kit (Clontech). The deletion of the *NcoI-HindIII* fragments (nucleotides 1293 to 1698) (Runt domain) of pEF- $\alpha$ A1 and pEF- $\alpha$ A2 resulted in the formation of pEF- $\alpha$ A1 $\Delta$ Runt and pEF- $\alpha$ A1(1-306) $\Delta$ Runt, respectively. pEF- $\alpha$ A1 $\Delta$ RuntN and pEF- $\alpha$ A1 $\Delta$ RuntC were constructed by eliminating the *NcoI-BstEII* and the *BstEII-HindIII* fragments, respectively, of pEF- $\alpha$ A1.

pEF- $\beta$ /MYH11 for the expression of the chimeric protein generated by *inv*(16) (22) was constructed as follows. Two PCRs were performed separately: (i) one with primer A (GGTATGGGCTGTCTGGAGTT) and primer B (GCTCATGGACCTCCATTTCTCCCGATG) and with human *PEBP2/CBF $\beta$*  cDNA (obtained from a human T-cell library with the mouse *PEBP2* cDNA as a probe) as a template and (ii) one with primer C (GGAAATGGAGGTCATGAGCTGAGAGAAG) and primer D (CGTGAAGCTGTCTCTGCAG) and with MYH-11 cDNA (23) as a template (24). The primers B and C represent the sequences of opposite strands spanning the breakpoint of the chimeric cDNA (22). The two PCR products were separated on a 1.5% agarose gel and recovered from the gel. These two PCR products were mixed, and secondary PCR was performed for 12 cycles in the absence of primers. Reaction conditions were 50 s at 94°C, 1 min at 50°C, and 2 min at 72°C. The recombinant PCR product was digested with *EcoT22I* present in the human *PEBP2/CBF $\beta$*  coding region and *XmaI* present in the MYH-11 coding region. The double-digested PCR product was used for the three-fragment ligation to make  $\beta$  $\beta$ /MYH. The DNA sequence of the PCR-amplified region of the artificially constructed chimeric cDNA was verified by dideoxy DNA sequencing. The *XbaI* fragment of  $\beta$  $\beta$ /MYH which contains the entire coding region was subcloned into the *XbaI* site of pEF-BOS from which the simian virus 40 replication origin was deleted (29).

**Preparation of the bacterial lysate and purification of *E. coli*-produced proteins.** *Escherichia coli* B21 (39, 45) was transformed by the bacterial expression plasmid pET $\alpha$ A1, pET $\beta$ , or pET $\alpha$ A1C17. The transformed cells grown in Luria-Bertani broth were incubated at 37°C in the presence of 1 mM isopropyl- $\beta$ -D-thiogalactopyranoside (IPTG) for 2 h. Cells were harvested and the proteins were extracted as follows (11). Cells were suspended in a buffer containing 50 mM Tris-HCl (pH 8.0), 0.5 mM EDTA, 0.4 M NaCl, 5 mM MgCl<sub>2</sub>, 5% (vol/vol) glycerol, 0.1 mM phenylmethylsulfonyl fluoride (PMSF), 0.1 mM dithiothreitol (DTT), and 1 mg of lysozyme per ml, incubated for 60 min on ice, and then subjected to two cycles of freezing and thawing. EDTA or Nonidet P-40 was added to the lysate at 1 mM or 0.5%, respectively, and the mixture was sonicated in a sonifier cell disrupter (UC100-D; Olympus, Tokyo, Japan). The lysate was centrifuged at 27,000 rpm in a 60Ti rotor (Beckman) at 4°C for 60 min, and the supernatant was taken as a soluble fraction. The pellet was resuspended in a buffer containing 50 mM Tris-HCl (pH 8.0), 1% (vol/vol) Triton X-100, 6 M urea, 5% glycerol, 0.1 mM PMSF, and 0.1 mM DTT. The mixture was kept on ice for 90 min and centrifuged at 39,000 rpm in a 60Ti rotor (Beckman) at 4°C for 90 min. The supernatant was collected as an insoluble fraction. Most of the  $\alpha$ A1 and  $\alpha$ A1C17 proteins were found in an insoluble fraction, whereas the  $\beta$ 2 protein was in a soluble fraction.

*E. coli* BL21 transformed with pQE9- $\alpha$ A1 for the expression of histidine-tagged  $\alpha$ A1 was incubated in the presence of 0.5 mM IPTG for 2 h and lysed in a buffer containing 6 M guanidine-HCl (pH 8.0), 0.1 M sodium phosphate, 10 mM Tris, 1 mM PMSF, and 10 mM  $\beta$ -mercaptoethanol.  $\alpha$ A1 was purified with nickel-chelate affinity resin (Qiagen), according to the manufacturer's instructions. The eluted fraction was separated by sodium dodecyl sulfate (SDS)-12.5% polyacrylamide gel electrophoresis (PAGE). The gel was stained with 0.3 M CuCl<sub>2</sub> as described previously, and the band expected to contain  $\alpha$ A1 was excised. The elution of the protein from the gel, trichloroacetic acid precipitation, and denaturation and renaturation of the protein by dialysis were performed as described previously (15). *PEBP2 $\beta$ 2* expressed in *E. coli* was purified by a method described previously (33).

**Preparation of antisera.** Antisera against three *E. coli*-produced proteins were prepared. The immunogens used were the 35-kDa amino-terminal region of  $\alpha$ A1 (see Results for details), the carboxy-terminal 17-kDa region of  $\alpha$ A1 composed of 155 aa (from aa 359 through 513), and the entire  $\beta$ 2 protein. The *E. coli*-produced proteins were separated by SDS-12.5% PAGE (21). After electrophoresis, the gel was stained with 0.05% Coomassie brilliant blue for 15 min. The gel was destained with deionized water, and the band containing the induced protein was excised and crushed by passage through a 21-gauge needle three times. The crushed material suspended in phosphate-buffered saline (PBS) was mixed with an equal volume of Freund complete adjuvant (Difco). The emulsion was injected subcutaneously into Japan White rabbits or Syrian hamsters at multiple sites. The amount of antigen used for one immunization was 300 or 60  $\mu$ g of protein for a rabbit or a hamster, respectively. A booster injection with Freund incomplete adjuvant in this case was given at least three times at 2-week intervals. Blood was collected 2 weeks after the final injection. The antibody titers of the sera were monitored by enzyme-linked immunosorbent assay (ELISA) with *E. coli*-produced proteins as antigens. Rabbit anti- $\alpha$ A1N35 and rabbit anti- $\beta$ 2 were partially fractionated into immunoglobulin G1 (IgG1) and IgG2 subfractions as follows. IgG in the sera was precipitated by 50% saturated ammonium sulfate, dissolved in PBS, and dialyzed against a buffer containing 3 M NaCl and 1.5 M glycine (pH 8.9) and applied to an Affi-Gel protein A column (Bio-Rad) equilibrated with the same buffer. After a washing, IgG was eluted by 0.1 M sodium citrate (pH 6.0). This fraction, designated fraction 1, is considered to contain mainly the IgG1 subfraction. Fraction 2 was prepared from the precipitate in 50% saturated ammonium sulfate as follows. The precipitated IgG was dissolved in PBS, dialyzed against PBS, and applied to the column equilibrated with PBS. Fraction 2 was eluted by 0.1 M sodium citrate (pH 4.0), which was considered to contain mainly IgG2a and IgG2b subfractions.

**Preparation of nuclear extracts and whole-cell extracts.** Nuclear extracts were prepared from NIH 3T3 and Ha-*ras*-transformed NIH 3T3 cells according to a procedure described previously (42). Whole-cell extracts of COS-7 cells were prepared 40 h after DNA transfection by a freezing-thawing method as previously described (36). Whole-cell extracts were superior to nuclear extracts in terms of keeping the proteins from proteolytic degradation, presumably because of less manipulation during extraction.

**Western blot (immunoblot) analysis.** Whole-cell extracts or proteins purified from the bacterial lysate were separated by SDS-12.5% PAGE. Proteins in the gel were transferred electrophoretically (at 40 V for 12 h) onto a nitrocellulose membrane (Schleicher & Schuell). The blocking reaction was performed by shaking the membrane for 1 h in Tris-buffered saline (TBS; 20 mM Tris-HCl [pH 7.6], 137 mM NaCl) containing 0.1% Tween 20 and 5% nonfat dry milk. The membrane was incubated for 1 h with the 4,000-fold-diluted primary antisera in TBS containing 0.1% Tween 20. After a washing in TBS containing 0.1% Tween 20, the membrane was reacted for 1 h with the 1,000-fold-diluted horseradish peroxidase-conjugated goat anti-rabbit IgG (Jackson ImmunoResearch Laboratories, Inc.) or rabbit anti-hamster IgG (Rockland, Inc.). Proteins were visualized by the standard method (41). For staining the gel, a two-dimensional silver stain II kit (Daiichi Kagaku, Tokyo, Japan) was used.

**EMSA.** The nuclear extract containing 10  $\mu$ g of proteins was mixed with various amounts of antiserum and adjusted to 5  $\mu$ l with buffer D containing 100

mM KCl (7). Electrophoretic mobility shift assay (EMSA) was performed essentially as described previously (42). Briefly, the mixture was incubated on ice for 20 min, and then a mixture of a 1 nM concentration of the DNA probe ( $2.0 \times 10^6$  cpm/pmol) in 5  $\mu$ l of a buffer containing 40 mM *N*-2-hydroxyethylpiperazine-*N'*-2-ethanesulfonic acid (HEPES)-KOH, (pH 7.6), 8% (wt/vol) Ficoll, 100 mM KCl, 1.5  $\mu$ g of poly(dI-dC), 4 mM EDTA, and 2 mM DTT was added. The incubation was continued at room temperature for 30 min. Samples were analyzed on 6% nondenaturing polyacrylamide (60:1, acrylamide-bisacrylamide) gels. The DNA probe used was  $\Delta$ F9-5000 (5'-AACTGACCGCAGCTGGCCGTGCGA-3') end labeled with  $^{32}$ P by T4 polynucleotide kinase (40).

**Immunofluorescence labeling.** NIH 3T3 cells were seeded 24 h prior to transfection at  $2 \times 10^5$  cells per 10-cm-diameter dish, in which glass coverslips were placed. Forty hours after plasmid DNA transfection, the cells were fixed in 3.7% (wt/vol) formaldehyde in PBS for 20 min. The cells were rinsed in PBS and then permeabilized with 0.1% (vol/vol) Nonidet P-40 in PBS for 10 min. A blocking reaction was done in PBS containing 5% (vol/vol) normal goat serum (Gibco BRL) and 1 mg of bovine serum albumin fraction V (Sigma) per ml for 60 min. The cells were incubated with the primary antisera (100-fold-diluted anti- $\alpha$ A1N35 or 200-fold-diluted rabbit or hamster anti- $\beta$ 2 in a blocking solution) for 60 min. The cells were rinsed in PBS and were further incubated with the secondary antisera (80-fold-diluted fluorescein isothiocyanate [FITC]-conjugated goat anti-rabbit IgG, IgA, and IgM [Binding Site, Birmingham, United Kingdom] or 200-fold-diluted tetramethylrhodamine isothiocyanate-conjugated goat anti-hamster IgG [E. Y. Laboratories, Inc., San Mateo, Calif.]) for 60 min. After a washing in PBS, coverslips were mounted on microscopic slides with a buffered glycerol mounting medium (BBL, Cockeysville, Md.). All the above procedures were performed at room temperature. The cells were visualized and photographed with a fluorescence microscope (Zeiss) with a 40 $\times$  objective lens. For double labeling, the mixture of anti- $\alpha$ A1N35 and hamster anti- $\beta$ 2 was used as the primary antiserum and the mixture of FITC-conjugated anti-rabbit goat IgG, IgA, and IgM and tetramethylrhodamine isothiocyanate-conjugated anti-hamster goat IgG was used as the secondary antiserum.

## RESULTS

**Specificities of the antisera raised against PEBP2 $\alpha$ A1 and PEBP2 $\beta$ 2.** Antiserum against *E. coli*-produced  $\alpha$ A1 was raised in rabbits. The  $\alpha$ A1 protein produced in *E. coli* readily degrades and results in a stable fragment of about 35 kDa (35). This fragment lacks the C-terminal portion of  $\alpha$ A1 (see below). This 35-kDa protein was used as an antigen to immunize rabbits. The antiserum produced will be referred to as anti- $\alpha$ A1N35. The C-terminal region of  $\alpha$ A1 from aa 359 to 513 was also produced in *E. coli*. The antiserum raised in rabbits against this C-terminal 17-kDa region will be referred to as anti- $\alpha$ A1C17. The antisera against the full-length  $\beta$ 2 produced in *E. coli* were raised in rabbits and hamsters. They will be referred to as rabbit anti- $\beta$ 2 and hamster anti- $\beta$ 2, respectively.

The specificities of the antisera were first tested by Western blotting with *E. coli*-produced proteins. Crude extracts of *E. coli* expressing  $\alpha$ A1 or the backbone vector were separated by SDS-PAGE and subjected to Western blot analysis with anti- $\alpha$ A1N35 and anti- $\alpha$ A1C17. As shown in Fig. 1, the extract of the  $\alpha$ A1-expressing cells, but not that of the control cells, generated multiple bands which react with anti- $\alpha$ A1N35 (compare lanes 1 and 2). The largest and one of the most prominent components has a molecular size of 60 kDa. An equally intense band migrates at 35 kDa. It is likely that the 60-kDa protein is the primary product of the  $\alpha$ A1 cDNA and that the 35-kDa protein is a stable intermediate of the proteolytically cleaved  $\alpha$ A1 protein. The rest of the multiple bands are considered to be degradation intermediates.

In parallel blots probed with anti- $\alpha$ A1C17 (Fig. 1, lanes 3 and 4), the 60-kDa protein and only a few slightly smaller fragments were detected. The results clearly demonstrate that the 60-kDa protein contains the C-terminal region but that most of the degradation intermediates including the 35-kDa fragment do not. The 35-kDa fragment used as an immunogen therefore must largely represent the amino N-terminal region of  $\alpha$ A1. It is not known, however, whether the 35-kDa fragment contains the intact N terminus of  $\alpha$ A1.

The reactivities of rabbit and hamster anti- $\beta$ 2, compared

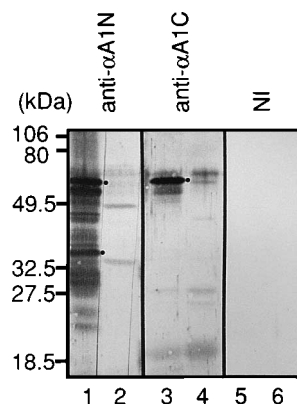


FIG. 1. Specificities of anti- $\alpha$ A1N35 and anti- $\alpha$ A1C17 as revealed by Western blot analysis. Crude extracts (insoluble fraction) of *E. coli* expressing  $\alpha$ A1 or backbone vector pET-3a-containing cells were separated by SDS-PAGE, and Western blot analysis was performed. The antisera used were anti- $\alpha$ A1N35 (anti- $\alpha$ A1N; lanes 1 and 2), anti- $\alpha$ A1C17 (anti- $\alpha$ A1C; lanes 3 and 4), and nonimmune serum (NI; lanes 5 and 6). Molecular mass standards were run in parallel lanes, and the positions of the markers are indicated on the left. The major components, the 60- and 35-kDa proteins, reactive with the antisera are indicated by dots.

with that of anti- $\alpha$ A1N35, were also examined by Western blotting as follows. In this case, the purified full-size  $\alpha$ A1 and  $\beta$ 2 proteins were run in seven parallel gels next to a set of unrelated proteins. Proteins in one of the gels were visualized by silver staining (Fig. 2, lanes 1 to 3).  $\alpha$ A1 and  $\beta$ 2 migrated as 60-kDa (lane 2) and 25-kDa (lane 3) proteins, respectively. Six unrelated proteins were present at comparable levels in lane 1. Anti- $\alpha$ A1N35 detected only  $\alpha$ A1 and did not react with  $\beta$ 2 or any of the unrelated proteins used (lanes 4 to 6). Rabbit and hamster anti- $\beta$ 2 reacted only with  $\beta$ 2 and not with  $\alpha$ A1 or any control proteins (lanes 10 to 12 and 16 to 18, respectively). None of the preimmune sera reacted with any proteins in the gels (lanes 7 to 9, 13 to 15, and 19 to 21). Anti- $\alpha$ A1C17 did not cross-react with  $\beta$ 2 either (data not shown).

The abilities of anti- $\alpha$ A1N35 and anti- $\beta$ 2 to detect the respective proteins expressed in COS-7 cells transfected with the expression plasmids for  $\alpha$ A1 and  $\beta$ 2 were then examined by Western blotting (Fig. 3). Whole-cell extracts of COS-7 cells transfected with  $\alpha$ A1 (lanes 1 and 6),  $\beta$ 1 (lanes 2 and 7),  $\beta$ 2 (lanes 3 and 8), and  $\beta$ 3 (lanes 4 and 9) expression plasmids were separated by SDS-PAGE and subjected to Western blot analysis. As shown in lane 1, anti- $\alpha$ A1N35 clearly detected the 60-kDa protein in transfected cells. A band of the 60-kDa protein was barely visible or was not detected in cells transfected with other plasmids (compare lane 1 with lanes 2 to 5). This means that the 60-kDa protein represents the product of exogenously introduced  $\alpha$ A1 expression plasmid and that the level of endogenously expressed  $\alpha$ A1, if any, is very low. Anti- $\alpha$ A1C17 also detected the  $\alpha$ A1 but not the  $\beta$  proteins (data not shown).

In the case of hamster anti- $\beta$ 2, the 25-kDa protein was clearly detected in cells transfected with  $\beta$ 1 and  $\beta$ 2 expression plasmids (Fig. 3, lanes 7 and 8, respectively). The size difference (0.5 kDa) between the two proteins was not recognizable under the conditions used. In the cells transfected with  $\beta$ 3 plasmid, 25- and 20-kDa proteins were detected (lane 9). The 20-kDa protein is expected to be  $\beta$ 3. Hamster anti- $\beta$ 2 also detected a relatively low level of the 25-kDa protein in untransfected cells (lane 10) and  $\alpha$ A1 plasmid-transfected cells (lane 6). We infer that the 25-kDa band present at lower levels

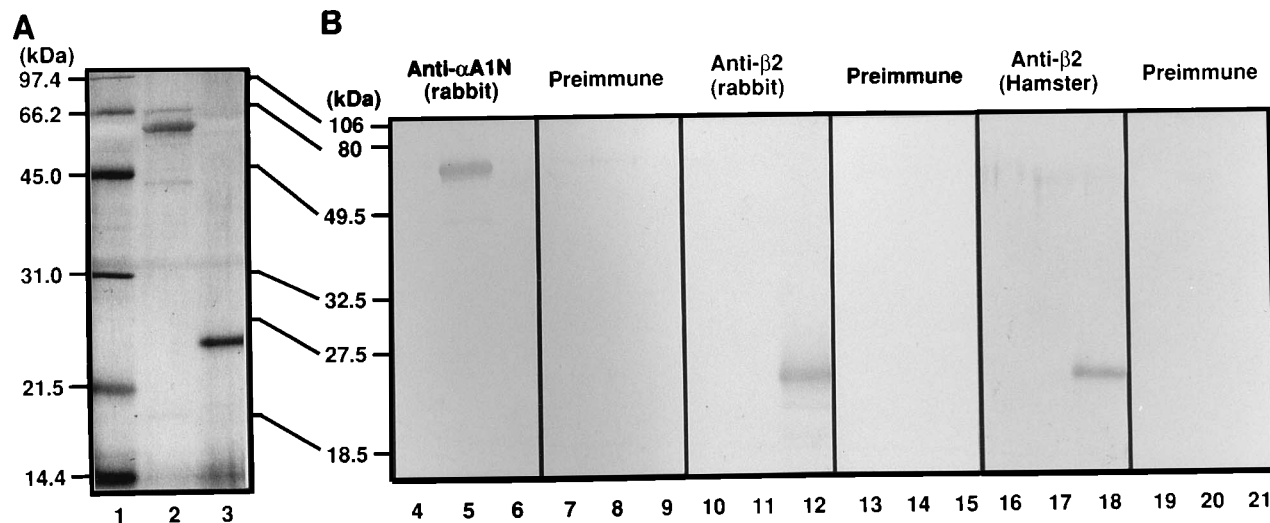


FIG. 2. Specificities of antisera as revealed by Western blot analysis. (A) Silver staining of a 12.5% polyacrylamide gel after SDS-PAGE of bacterially expressed proteins. Lane 1, 0.1  $\mu$ g of SDS-PAGE molecular mass standards (low range [14,000 to 97,400 Da]; Bio-Rad); lane 2, 1.1  $\mu$ g of gel-purified, histidine-tagged PEBP2 $\alpha$ A1 (see Materials and Methods); lane 3, 0.4  $\mu$ g of purified PEBP2 $\beta$ 2. Molecular mass standard sizes are indicated on the left. Prestained molecular mass standards (low range [~18,500 to 106,000 Da]; Bio-Rad) were also run in a parallel lane, and the position of each standard is indicated on the right. (B) Immunoblots of six independent gels run in parallel, each containing the same amounts of the proteins in the same order as in panel A. The blots were probed with anti- $\alpha$ A1N35 (lanes 4 to 6), rabbit anti- $\beta$ 2 (lanes 10 to 12), or hamster anti- $\beta$ 2 (lanes 16 to 18) as well as with the respective preimmune sera (lanes 7 to 9, 13 to 15, and 19 to 21, respectively) and were then treated with peroxidase-coupled goat anti-rabbit (lanes 4 to 15) or anti-hamster (lanes 16 to 21) IgG. The positions of prestained molecular mass standards run in a parallel lane are indicated on the left.

in lanes 6, 9, and 10 likely represents the endogenous  $\beta$  protein (either  $\beta$ 1 or  $\beta$ 2 or a mixture of the two).

**Immunological verification of molecular relatedness between PEBP2 and PEBP3.** PEBP2 was originally identified in NIH 3T3 cells as a protein which binds to the PEA2 site of the A core of the polyomavirus enhancer, as determined by EMSA (42). PEBP3 has the same DNA-binding specificity as PEBP2 but migrates faster than PEBP2 in EMSA and is often found in Ha-*ras*-transformed NIH 3T3 cells (42). PEBP3 was considered to be either a proteolytically degraded form of PEBP2 or a form which has lost a component of PEBP2. When cDNA cloning of PEBP2 was attempted, the PEBP3 form was purified to obtain partial amino acid sequences. The antisera used in the present study were raised against the protein products of these cDNAs. Therefore, we first tested whether antisera that we obtained would react with PEBP2 and PEBP3 in EMSA.

Figure 4, lane 1, shows PEBP2 from NIH 3T3 cells as detected by EMSA. The band was eliminated by a specific competitor (lane 2) but not by a mutated version (lane 3). The band was effectively eliminated in the presence of both anti- $\alpha$ A1N35 and anti- $\alpha$ A1C17 (lanes 5 and 6). Nonimmune serum did not react with the protein (lane 4). The results clearly demonstrated that PEBP2 in NIH 3T3 cells contains the polypeptide closely related to the N-terminal as well as C-terminal portions of  $\alpha$ A1. We reported earlier that NIH 3T3 cells express both the  $\alpha$ A and  $\alpha$ B genes (4, 35). The result suggests that anti- $\alpha$ A1N35 and anti- $\alpha$ A1C17 react with both  $\alpha$ A1 and  $\alpha$ B1 (see below). PEBP3 from Ha-*ras*-transformed NIH 3T3 cells (lane 11) also reacted well with anti- $\alpha$ A1N35 (compare lanes 14 and 15). In this case, however, no reaction with anti- $\alpha$ A1C17 was observed (lane 16). The results indicated that PEBP3 shares with PEBP2 a component antigenically related to the product of the  $\alpha$ A1 cDNA but lacks the region equivalent to the C-terminal region of  $\alpha$ A1. Conversion of PEBP2 to PEBP3, therefore, was suggested to be due to proteolysis of the C-terminal region of the  $\alpha$  polypeptide. At this moment, how-

ever, it is not clear whether PEBP3 contains the intact N terminus of  $\alpha$ A1.

Figure 4 also shows that rabbit anti- $\beta$ 2 can react with both PEBP2 (lanes 7 to 10) and PEBP3 (lanes 17 to 20). Thus, it is clear that PEBP2 and PEBP3 contain a component antigenically related to the product of the  $\beta$ 2 cDNA. All these results are consistent with our original assumption that PEBP3 is derived from PEBP2. In the above experiment, we noticed that the reactivity of anti- $\beta$ 2 with PEBP2 and PEBP3 was much weaker than those of anti- $\alpha$ A1N35 and anti- $\alpha$ A1C17 (lanes 7 to 10 and lanes 17 to 20, respectively), despite the fact that anti- $\alpha$ A1N35 and rabbit and hamster anti- $\beta$ 2 have comparable antibody titers in ELISA, Western blot, and immunofluores-

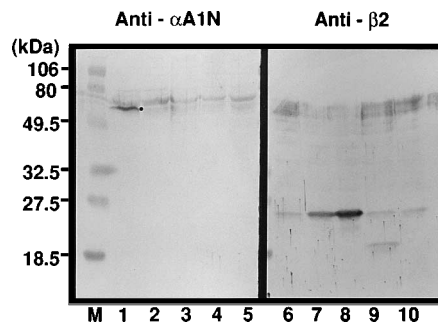


FIG. 3. Specificities of anti- $\alpha$ A1N35 and hamster anti- $\beta$ 2 as revealed by Western blot analysis with extracts from transfected COS-7 cells. COS-7 cells ( $10^6$  per dish, with a total of three dishes per plasmid) were transfected with expression plasmids for the  $\alpha$ A1 and the  $\beta$  proteins, and whole-cell extracts were prepared and subjected to Western blot analysis. A total of 15  $\mu$ g of the whole-cell extract per lane was used. Lanes 1 and 6, pEF- $\alpha$ A1; lanes 2 and 7, pEF- $\beta$ 1; lanes 3 and 8, pEF- $\beta$ 2; lanes 4 and 9, pEF- $\beta$ 3; lanes 5 and 10, pEF-BOS. The blots were probed with rabbit anti- $\alpha$ A1N35 (Anti- $\alpha$ A1N) or hamster anti- $\beta$ 2. Lane M, molecular mass standards (sizes of the marker proteins are indicated on the left). The  $\alpha$ A1 protein is indicated by a dot.

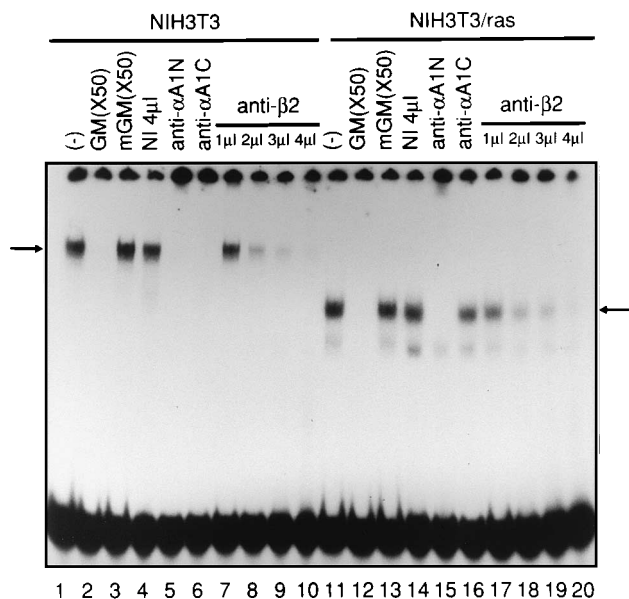


FIG. 4. Reactivities of anti- $\alpha$ A1N35, anti- $\alpha$ A1C17, and rabbit anti- $\beta$ 2 to PEBP2 and PEBP3, as examined by EMSA. Nuclear extracts of NIH 3T3 cells (lanes 1 to 10) and Ha-*ras*-transformed NIH 3T3 cells (lanes 11 to 20) were subjected to EMSA. The positions of the authentic PEBP2 and PEBP3 are indicated by arrows on the left and right, respectively. The 24-mer oligonucleotides (GM, GGAGTTCTGTGGTCACCATTACGC) representing the granulocyte-macrophage colony-stimulating factor promoter containing the PEBP2 site (nucleotides -64 to -58 [12, 26]) (lanes 2 and 12) or its mutated version (mGM, GGAGTTCTGGCGTCACCATTACGC) (lanes 3 and 13) were used as competitors at a 50-fold molar excess (X50). Four microliters of antisera was added to the reaction mixtures as indicated. When smaller amounts are indicated, nonimmune serum was added to make 4  $\mu$ l. Lanes 4 and 14, nonimmune serum (NI); lanes 5 and 15, anti- $\alpha$ A1N35 (anti- $\alpha$ A1N); lanes 6 and 16, anti- $\alpha$ A1C17 (anti- $\alpha$ A1C); lanes 7 to 10 and 17 to 20, anti- $\beta$ 2. (-), no competitors or antisera added.

cence assays. Essentially the same results were obtained with hamster anti- $\beta$ 2 (data not shown). One possible explanation for this discrepancy would be that the  $\beta$  protein is wrapped by the  $\alpha$  protein. However, the  $\beta$ 2 protein in the  $\alpha/\beta$  complex formed by either  $\alpha$ A1(1-226) or  $\alpha$ A1(94-306) (see Fig. 5 for the structure), which lack the region downstream or upstream, respectively, of the Runt domain, showed a similar level of reactivity to the antiserum (data not shown). The  $\beta$  protein may undergo conformational changes in the heterodimer complex so as to reduce its apparent antigenicity. Further studies are required to clarify this observation.

**Reactivities of the antisera to local domains of PEBP2 $\alpha$  and PEBP2 $\beta$ .** For use in the subsequent characterization and in situ labeling of PEBP2 $\alpha$  and PEBP2 $\beta$ , the reactivities of the antisera obtained above were examined in further detail with various deletion constructs of  $\alpha$  and  $\beta$ , as shown in Fig. 5. To verify that proteins of expected sizes are synthesized from these deletion constructs, the plasmids capable of expressing these constructs were transfected into COS-7 cells, and whole-cell extracts were subjected to Western blot analysis (Fig. 6). In all cases except for  $\alpha$ A1(94-513) and  $\alpha$ A1(94-226), the products of the expected sizes were detected by anti- $\alpha$ A1N35 (Fig. 6A).  $\alpha$ A1(94-513) was detected by anti- $\alpha$ A1C17, and its size was as expected (Fig. 6A, lane 15). A significant fraction of antibodies in anti- $\alpha$ A1N35, therefore, appeared to be directed against the N-terminal region of  $\alpha$ A1. Although  $\alpha$ A1(94-306) was detected by anti- $\alpha$ A1N35, it must have been detected, presumably because it accumulated in larger amounts than

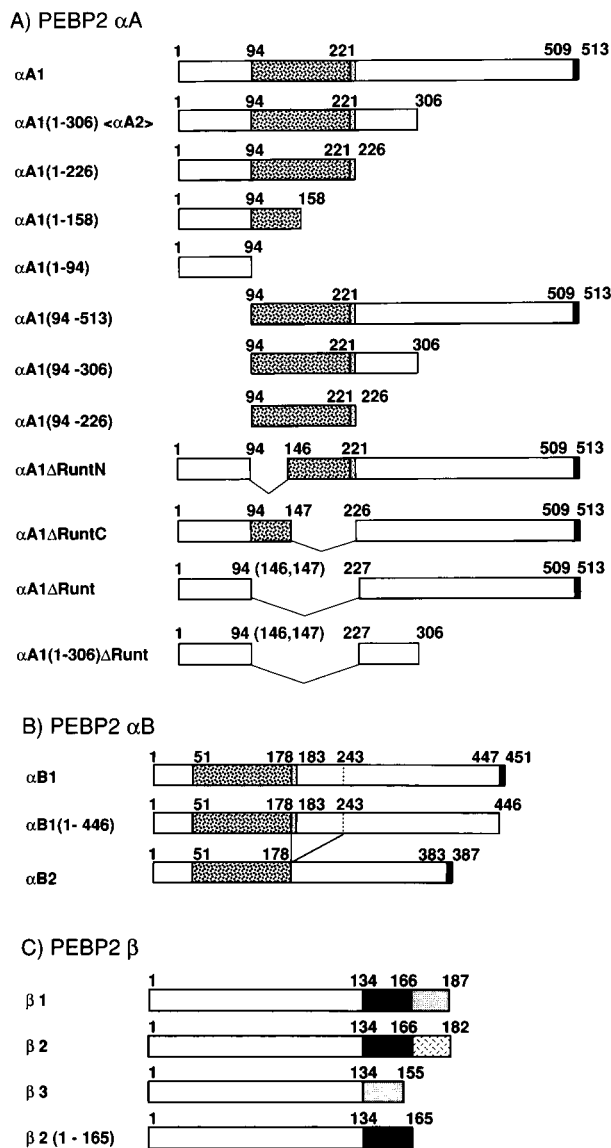


FIG. 5. Schematic representation of the full-length and deletion derivatives of PEBP2 $\alpha$ A (A), PEBP2 $\alpha$ B (B), and PEBP2 $\beta$  (C). (A and B) Stippled boxes represent the Runt domain. Narrow, filled boxes at the C-terminal end of some of the constructs represent the conserved 5 aa, VWRPY. (C) The C-terminal regions of PEBP2 $\beta$  isoforms indicated by different coloration show the sequence variations generated by alternative splicing. The regions indicated by the same color represent the same amino acid sequences.

$\alpha$ A1(94-513) (see below).  $\alpha$ A1(94-226) representing the Runt domain was detected neither by anti- $\alpha$ A1N35 nor by anti- $\alpha$ A1C17 (data not shown). We found subsequently that it was difficult to raise the antiserum against the Runt domain. Since the Runt domain is evolutionarily highly conserved, it is likely that it is not strongly immunogenic. We confirmed, however, that  $\alpha$ A1(94-226) generated a fast-migrating band in EMSA which was within the expected mobility (data not shown). There was a tendency that C-terminally truncated proteins except for  $\alpha$ A1(1-94) were produced in larger amounts. This phenomenon is most likely due to the fact that the C-terminal regions of the  $\alpha$  polypeptides contain the PEST sequences (38) and are extremely susceptible to proteolytic degradation (35).  $\alpha$ B1(1-446) was indistinguishable from  $\alpha$ B1 under the condi-

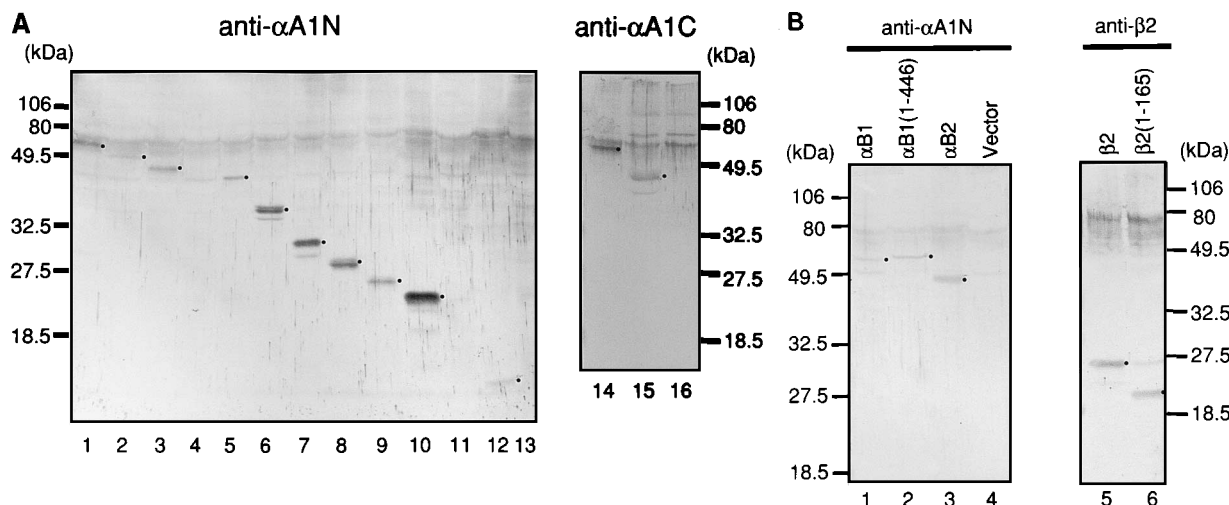


FIG. 6. Products of deletion constructs of PEBP2 $\alpha$ 1 cDNAs (A) or PEBP2 $\alpha$ B1, PEBP2 $\alpha$ B2, and PEBP2 $\beta$ 2 cDNAs (B) as revealed by Western blotting. (A) COS-7 cells were transfected with expression plasmids for the deletion mutants of  $\alpha$ A1 shown in Fig. 5, and whole-cell extracts were analyzed by Western blots probed with anti- $\alpha$ A1N35 (anti- $\alpha$ A1N; lanes 1 to 13) or anti- $\alpha$ A1C17 (anti- $\alpha$ A1C; lanes 14 to 16). (B) The products of  $\alpha$ B1,  $\alpha$ B1(1-446), and  $\alpha$ B2 were detected by anti- $\alpha$ A1N35 (anti- $\alpha$ A1N; lanes 1 to 3), and the products of  $\beta$ 2 and  $\beta$ 2(1-165) were detected by rabbit anti- $\beta$ 2 (lanes 5 and 6). The protein products of the transfected plasmids are indicated by dots. The apparent masses (calculated molecular masses) of the products were as follows: (A)  $\alpha$ A1 (lane 1), 60 (55.8) kDa;  $\alpha$ A1 $\Delta$ RuntN (lane 2), 50 (50.2) kDa;  $\alpha$ A1 $\Delta$ RuntC (lane 3), 45 (46.9) kDa;  $\alpha$ A1(94-513) (lane 4), undetectable (45.7 kDa);  $\alpha$ A1 $\Delta$ Runt (lane 5), 42 (41.4) kDa;  $\alpha$ A1(1-306) (lane 6), 36 (33.6) kDa;  $\alpha$ A1(1-226) (lane 7), 31 (24.8) kDa;  $\alpha$ A1(94-306) (lane 8), 28 (23.6) kDa;  $\alpha$ A1(1-306) $\Delta$ Runt (lane 9), 26 (19.2) kDa;  $\alpha$ A1(1-154) (lane 10), 24 (17.0) kDa;  $\alpha$ A1(94-226) (lane 11), undetectable (14.8 kDa);  $\alpha$ A1(1-94) (lane 12), 13 (10.2) kDa; pEF-BOS (lane 13), vector;  $\alpha$ A1 (lane 14), 60 (55.8) kDa;  $\alpha$ A1(94-513) (lane 15), 46 (45.7) kDa;  $\alpha$ A1(1-226) (lane 16), undetectable (24.8 kDa); (B)  $\alpha$ B1 (lane 1), 55 (48.6) kDa;  $\alpha$ B1(1-446) (lane 2), 55 (47.9) kDa;  $\alpha$ B2 (lane 3), 46 (41.3) kDa; pEF-BOS (lane 4), vector;  $\beta$ 2 (lane 5), 25 (21.5) kDa; and  $\beta$ 2(1-165) (lane 6), 21 (19.7) kDa. The positions of the protein mass markers run in parallel lanes are indicated in each panel.

tions used (Fig. 6B, compare lanes 1 and 2).  $\beta$ 2(1-165) showed the expected size (Fig. 6B, lane 6); we assumed that a faint band in lane 6 comigrating with  $\beta$ 2 represents the endogenous  $\beta$  protein.

**Immunofluorescence labeling of the cells transfected with the PEBP2 $\alpha$  and PEBP2 $\beta$  cDNAs.** To examine the subcellular localization of the  $\alpha$  and  $\beta$  subunits of PEBP2 and to identify the sequence elements in these subunits which dictate the localization, various deletion constructs listed in Fig. 5 were transfected into NIH 3T3 cells and the protein products were detected by labeling with fluorescein-conjugated antibodies. Figure 7b shows several cells under the phase microscope in the culture transfected with the  $\alpha$ A1 expression plasmid. Only one of them is successfully transfected by the plasmid, as revealed in Fig. 7a, which shows immunofluorescence labeling of only one cell by anti- $\alpha$ A1N35. A strong fluorescence in the nucleus, except for nucleoli, is evident. Under the conditions used, untransfected cells were not labeled and looked similar to the cells in the upper part of Fig. 7a, indicating that the endogenous  $\alpha$  proteins in NIH 3T3 cells were below the level of detection. This labeling experiment clearly demonstrated that  $\alpha$ A1 is a nuclear protein. When the C-terminal 207 aa were deleted, the product,  $\alpha$ A1(1-306), became detectable in the cytoplasm, although the greater fraction was still present in the nucleus (Fig. 7c). This result suggested that at least a part of the nuclear localization signal was located within the last 207-aa region of  $\alpha$ A1. Further C-terminal truncation to aa 226, which is the C-terminal border of the Runt domain [ $\alpha$ A1(1-226)], did not change the localization pattern any further (Fig. 7d). The C-terminally truncated  $\alpha$ A1 containing only a half of the Runt domain [ $\alpha$ A1(1-158)], which lacks the abilities both to associate with the  $\beta$  subunit and to bind to DNA, was mostly localized to the cytoplasm, although some nuclear fluorescence was still detected (Fig. 7e). The polypeptide containing only the N-terminal 94 aa [ $\alpha$ A1(1-94)] was no longer translocated into the nucleus at all (Fig. 7f). In accordance with this obser-

vation, the deletion of the N-terminal 93 aa [ $\alpha$ A1(94-513)] did not affect the nuclear localization of  $\alpha$ A1 (Fig. 7g). Once again, the deletion of the last 207 aa from  $\alpha$ A1(94-513) to make  $\alpha$ A1(94-306) resulted in the partial loss of nuclear translocation ability (Fig. 7h). Therefore, it appeared that there was a second element determining the nuclear localization somewhere within the Runt domain, and the N-terminal 93 aa did not contain such an element.

To further localize the putative nuclear localization signal within the Runt domain, three more deletion constructs were tested. The internal deletion of the N- or C-terminal half of the Runt domain of  $\alpha$ A1 ( $\alpha$ A1 $\Delta$ RuntN and  $\alpha$ A1 $\Delta$ RuntC, respectively) indeed changed the localization pattern. In both cases, the proteins were present both in the nucleus and in the cytoplasm (Fig. 7i and j, respectively). In these cases, larger fractions appeared to be in the nucleus. Removal of the Runt domain completely from  $\alpha$ A1 ( $\alpha$ A1 $\Delta$ Runt) made more of the fraction stay in the cytoplasm (Fig. 7k). The  $\alpha$ A1 proteins devoid of the intact Runt domain are unable to bind to the  $\beta$  protein. Therefore, these results also indicate that the  $\alpha$  protein alone without binding to the  $\beta$  protein can be translocated into the nucleus. As shown above,  $\alpha$ A1(1-306) does not contain one of the nuclear localization signals. Interestingly, removal of the Runt domain from  $\alpha$ A1(1-306) to make  $\alpha$ A1(1-306) $\Delta$ Runt did not change it completely to a cytoplasmic protein (Fig. 7l), suggesting that the signal in the C-terminal region extends further towards the N terminus into the region between 226 and 306.

The rabbit anti- $\alpha$ A1N35 cross-reacted with the  $\alpha$ B protein. The full-size  $\alpha$ B1-transfected cells showed nuclear staining indistinguishable from that of  $\alpha$ A1 (Fig. 7m). The deletion of 5 aa, VWRPY, from the C-terminal end of  $\alpha$ B1, which is 100% conserved from *Drosophila runt* protein to mammalian  $\alpha$ A1 and  $\alpha$ B1 proteins (35), did not change the pattern, indicating that this evolutionarily conserved sequence is not involved in the nuclear accumulation of the protein (Fig. 7n). The  $\alpha$ B2

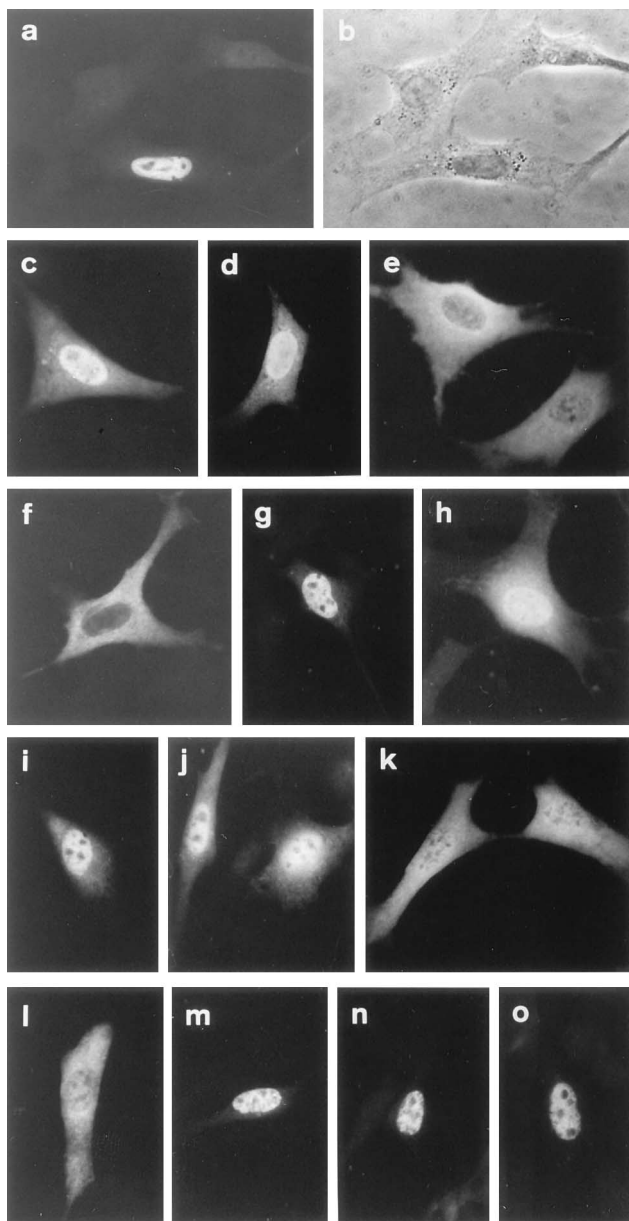


FIG. 7. Immunofluorescence labeling of the  $\alpha$ A and  $\alpha$ B proteins and their deletion derivatives expressed in NIH 3T3 cells. Transfected plasmids are as follows:  $\alpha$ A1 (a and b),  $\alpha$ A1(1-306) (c),  $\alpha$ A1(1-226) (d),  $\alpha$ A1(1-158) (e),  $\alpha$ A1(1-94) (f),  $\alpha$ A1(94-513) (g),  $\alpha$ A1(94-306) (h),  $\alpha$ A1 $\Delta$ RuntN (i),  $\alpha$ A1 $\Delta$ RuntC (j),  $\alpha$ A1 $\Delta$ Runt (k),  $\alpha$ A1(1-306) $\Delta$ Runt (l),  $\alpha$ B1 (m),  $\alpha$ B1(1-446) (n), and  $\alpha$ B2 (o). (a and c through o) Immunofluorescence labeling with anti- $\alpha$ A1N35; (b) phase-contrast photomicrograph. Panels a and b are the same field.

protein is identical to  $\alpha$ B1 except for the internal deletion of a 64-aa region located adjacent to the Runt domain at the C-terminal side (2). This 64-aa region contains a cluster of basic amino acid sequence which is highly homologous to the corresponding region of  $\alpha$ A1. Figure 7o revealed that the fluorescence pattern of  $\alpha$ B2 is indistinguishable from that of the full-size  $\alpha$ A1 or  $\alpha$ B1, indicating that the 64-aa region of  $\alpha$ B1 and, most likely, the 58-aa region (from aa 221 to 278) of  $\alpha$ A1, which corresponds to the 64-aa region of  $\alpha$ B1 (2), are not included in the nuclear localization signals. Hence, the basic amino acid clusters within this region are not involved in this

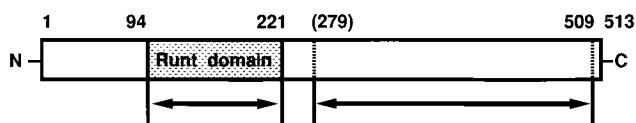


FIG. 8. Locations of the elements determining the nuclear accumulation in the  $\alpha$ A1 protein. The precise boundaries of the two elements are not known at present. Residue 279 in parentheses is considered to be equivalent to residue 242 of  $\alpha$ B1, which represents the C-terminal boundary of a small exon with 64 aa residues missing in  $\alpha$ B2 (2).

function. Figure 8 summarizes the results of this fluorescence labeling experiment. Some truncated proteins may have lost the ability to enter the nucleus not because they lost the required element but because they could not fold properly. The possible effects of abnormal protein folding will have to be studied in the future.

Subcellular localization of  $\beta$ 1,  $\beta$ 2, and  $\beta$ 3 was similarly examined with the hamster anti- $\beta$ 2 antiserum. As shown in Fig. 9A, the  $\beta$ 2 protein was present mainly in the cytoplasm. The  $\beta$ 1 protein also displayed a labeling pattern very similar to that shown in Fig. 9A. The  $\beta$ 3 protein which does not associate with the  $\alpha$  protein also showed a fluorescence pattern indistinguishable from those of  $\beta$ 1 and  $\beta$ 2. The  $\beta$ (1-165) polypeptide, which is equivalent to the part present in the chimeric protein generated by *inv*(16), also displayed the same cytoplasmic labeling pattern. In this case, too, endogenously expressed  $\beta$  protein was not detectable.

Failure to detect endogenously expressed PEBP2 $\alpha$  and PEBP2 $\beta$  proteins was due not only to low amounts of the proteins present in the cells but also to relatively high levels of nonspecific labeling of the cells by nonimmune sera as well as antisera. Since we detected endogenous  $\beta$  protein by Western blotting, we thought we should be able to detect at least the  $\beta$  protein by immunofluorescence labeling as well. We attempted to eliminate nonspecific labeling activities by partially fractionating the antisera. Fraction 1, which was thought to contain mainly the IgG1 subfraction, had a low antibody titer. However, it contained very low levels of nonspecific labeling activity. Fraction 2, which was considered to contain mainly the IgG2a and IgG2b subfractions, showed higher antibody titers but also contained high levels of nonspecific labeling activities. Therefore, fraction 1 was more useful for the present purpose. As shown in Fig. 9B, endogenous  $\beta$  protein labeled by fraction 1 of anti- $\beta$ 2 was also detected mainly in the cytoplasm. The  $\alpha$  protein could not be detected by fraction 1 of anti- $\alpha$ A1N35, probably because the  $\alpha$  protein is unstable and does not accumulate in amounts large enough to be easily detected.

**Effects of coexpressed  $\alpha$ A1 on the localization of  $\beta$ .** The observation shown in Fig. 9 that the  $\beta$  protein is localized mainly in the cytoplasm raises an intriguing question on the regulation of PEBP2 site-dependent transcription. It is presumed that the  $\beta$  protein functions in the nucleus in combination with the  $\alpha$  protein; the question is, how would the translocation of the  $\beta$  protein into the nucleus be regulated?

The expression plasmids for  $\alpha$ A1 and  $\beta$ 2 were cotransfected into cells, and subcellular localization of each protein was determined by double labeling.  $\alpha$ A1 was detected by rabbit anti- $\alpha$ A1N35 and FITC-conjugated anti-rabbit IgG. As expected,  $\alpha$ A1 displayed a typical nuclear fluorescence (Fig. 10a).  $\beta$ 2 was detected by hamster anti- $\beta$ 2 and rhodamine-conjugated anti-hamster IgG. Surprisingly, the  $\alpha$ A1 and  $\beta$ 2 proteins did not colocalize, and  $\beta$ 2 was present mainly in the cytoplasm (Fig. 10b). Thus, cotranslated  $\alpha$ A1 and  $\beta$ 2 do not appear to associate readily to form a heterodimer, although

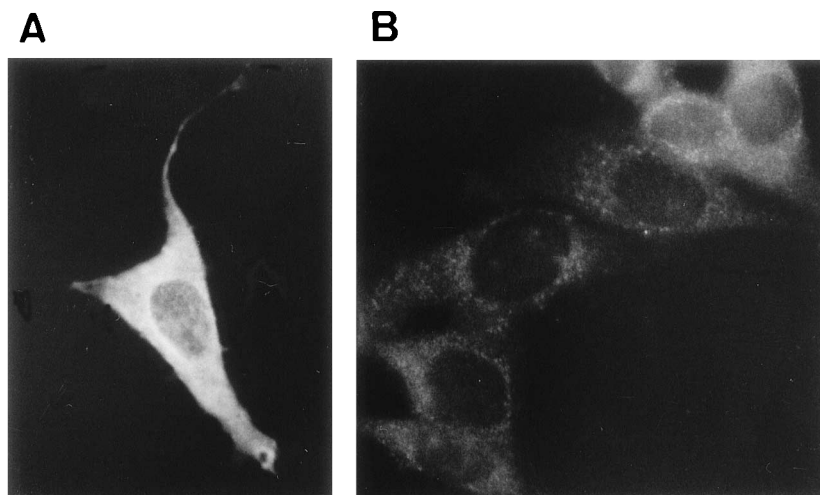


FIG. 9. Immunofluorescence labeling of  $\beta 2$  with rabbit anti- $\beta 2$  expressed in NIH 3T3 cells. (A) NIH 3T3 cells transfected with pEF- $\beta 2$ . Under the conditions used, untransfected cells were not detectable. (B) Untransfected NIH 3T3 cells. Fraction 1 of rabbit anti- $\beta 2$  serum (see Materials and Methods) was used.

the presence of some proportion of  $\beta 2$  in the nucleus cannot be ruled out, since an immunofluorescence labeling pattern does not give a precise quantitative estimation of the protein distribution. However, when the N-terminally truncated  $\alpha A1$  [ $\alpha A1(94-513)$ ] was cotransfected with  $\beta 2$ , the  $\alpha$  and  $\beta$  proteins did colocalize to the nucleus (Fig. 10c and d). This dramatic change in the localization pattern of  $\beta 2$  strongly suggests that the N-terminal region of  $\alpha A1$  somehow prevents a free association of  $\alpha A1$  with  $\beta 2$ . This also implies that  $\beta 2$  is translocated into the nucleus passively by binding to  $\alpha A1$ .

Similar colocalization of  $\alpha A1$  and  $\beta 2$  in the nucleus was observed when the C-terminally truncated  $\alpha A1$  [ $\alpha A1(1-224)$ ] and  $\beta 2$  were cotransfected (Fig. 10e and f). It appeared, therefore, that the regions both upstream and downstream of the Runt domain are inhibitory to the binding of  $\beta 2$  to  $\alpha A1$ . The N-terminal region of  $\alpha A1$  [ $\alpha A1(1-94)$ ] was never translocated into the nucleus (Fig. 10g). In this case,  $\beta 2$  was also present in the cytoplasm (Fig. 10h).

**PEBP2/CBF $\beta$ -MYH11 colocalizes with  $\alpha A1$  to the nucleus more readily than  $\beta 2$ .** The chimeric protein PEBP2/CBF $\beta$ -MYH11, which was generated as a result of the inversion of chromosome 16 observed in acute myeloid leukemia (22), contains the region of the  $\beta$  protein necessary and sufficient for dimerizing with the  $\alpha$  protein (35). Since this chimeric protein is a structurally altered  $\beta$  protein, we examined whether it would be translocated into the nucleus more readily than the normal  $\beta$  protein.

PEBP2/CBF $\beta$ -MYH11, when expressed alone, localized to the cytoplasm (Fig. 11a). When PEBP2/CBF $\beta$ -MYH11 and  $\alpha A1$  were coexpressed, a substantial fraction of the chimeric protein colocalized with  $\alpha A1$  to the nucleus. Some fractions of these two proteins were also colocalized to the cytoplasm, including to the unknown structure, suggesting that these two proteins bound together (Fig. 11b and c). This is the only condition tested so far under which full-size  $\alpha A1$  stably localizes in the cytoplasm. The implication of the observations obtained by the double labeling whose results are shown in Fig. 10 and 11 will be discussed below.

## DISCUSSION

The present study revealed that the  $\alpha$  subunit of a new transcription factor, PEBP2, is a nuclear protein, while the  $\beta$

subunit is a cytoplasmic one. The  $\beta$  protein can be translocated into the nucleus when it is coexpressed with either the N- or C-terminally truncated  $\alpha$  protein. The full-size  $\alpha$  protein does not seem to associate with the  $\beta$  protein readily, while removal of the region upstream or downstream of the Runt domain appears to allow the  $\alpha$  protein to bind to the  $\beta$  protein *in vivo*. These results suggest that the mechanism by which the  $\alpha$  protein becomes receptive to the  $\beta$  protein represents the first step of a novel mechanism of transcriptional regulation employed by PEBP2.

Regulation of transcription at the level of nuclear translocation of transcription factors has been described for several transcription factors including Rel/ $\kappa B$  family proteins (5) and NF-AT (9, 31). The most extensively studied factor in this respect is NF- $\kappa B$ . In this case, an inhibitor protein, I $\kappa B$ , holds transcriptionally active the p50/p65 heterodimer of NF- $\kappa B$  in the cytoplasm. Upon stimulation of the cells to activate  $\kappa B$  site-dependent transcription, I $\kappa B$  is inactivated by phosphorylation, whereby p50/p65 is translocated into the nucleus. The mechanism of regulation involving PEBP2 will be completely different from this case and may represent a novel type, if the mechanism implied by the results of the present study is proved to be correct.

The result obtained in this study, that the full-size  $\alpha A1$  does not readily associate with the  $\beta$  protein *in vivo*, suggests that an important rate-limiting step of PEBP2 site-dependent transcription activation is at the level of association between the two subunits, presumably taking place in the cytoplasm. Although the  $\alpha$  protein alone can enter the nucleus and it has been shown to bind to DNA *in vitro* poorly, this weak DNA binding may not be meaningful physiologically in terms of transcription activation. In order for PEBP2 to function, therefore, the  $\alpha/\beta$  heterodimer must be formed. The heterodimerization appeared to have taken place readily when the N- or C-terminally truncated  $\alpha$  polypeptides were used. The results imply that the polypeptides flanking the Runt domain prevent the  $\beta$  protein from associating with the Runt domain. Under physiological conditions, this inhibitory effect of the flanking regions, when necessary, may be relieved by some sort of protein modification. An attractive model would be that the protein modification of the  $\alpha$  polypeptide takes place after the polypeptide receives a signal to activate PEBP2 site-dependent transcription, possibly from cell surface receptors, to change



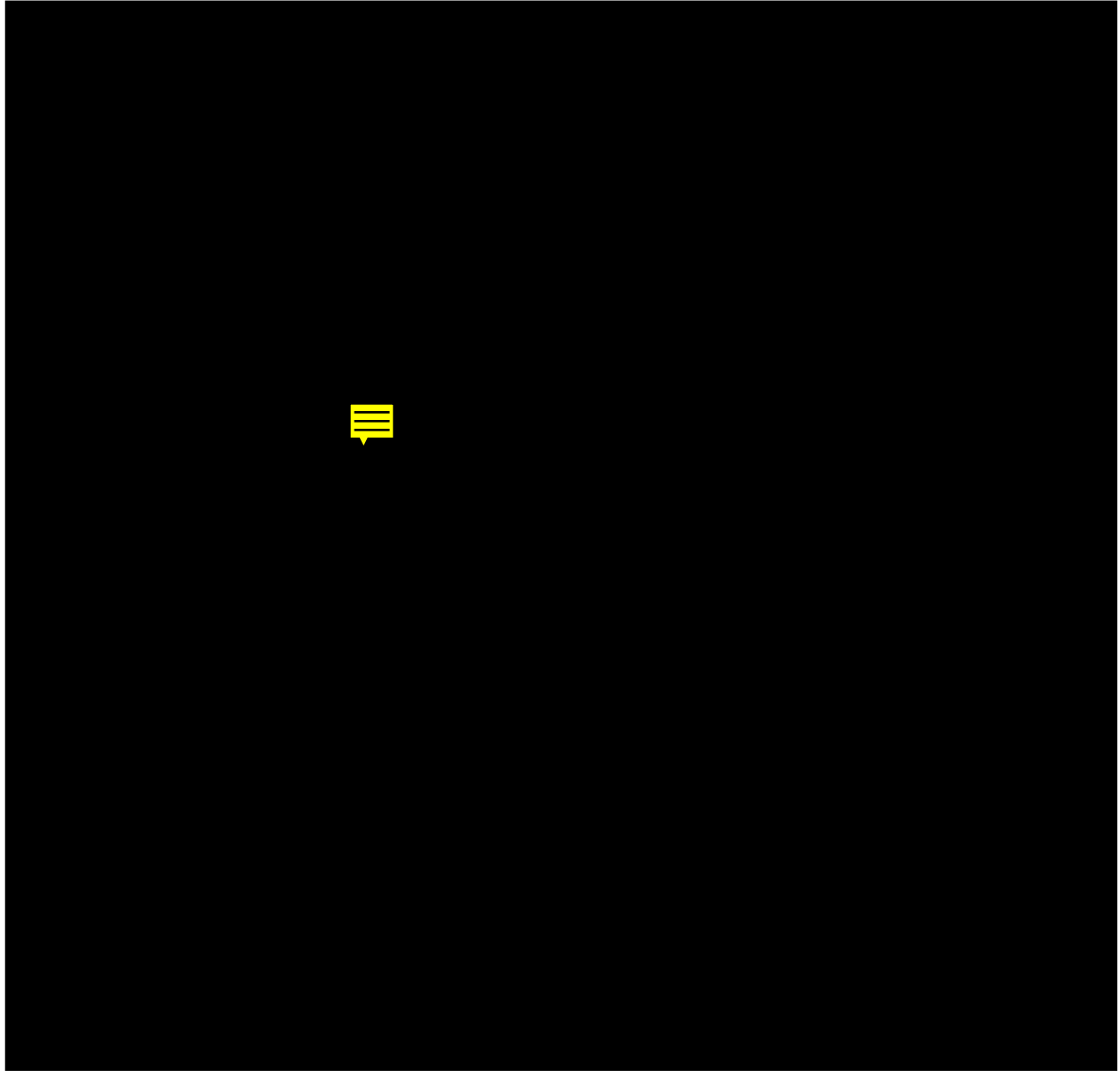


FIG. 10. Double fluorescence labeling of the NIH 3T3 cells cotransfected with the expression plasmids for  $\alpha$ A1 or its deletion derivatives and  $\beta$ 2. (a and b)  $\alpha$ A1 and  $\beta$ 2 plasmids; (c and d)  $\alpha$ A1(94-513) and  $\beta$ 2 plasmids; (e and f)  $\alpha$ A1(1-226) and  $\beta$ 2 plasmids; (g and h)  $\alpha$ A1(1-93) and  $\beta$ 2 plasmids; (a, c, e, and g) detection of FITC-conjugated antibody against rabbit IgG with a 495-nm-wavelength filter; (b, d, f, and h) detection of rhodamine-conjugated antibody against hamster IgG with a 555-nm-wavelength filter.

the conformation of the  $\alpha$  protein in such a way as to associate with the  $\beta$  protein. There is also a possibility that the protein modification must occur on the  $\beta$  subunit moiety for this mechanism to operate. The heterodimer would then be translocated into the nucleus to activate target genes. Indeed, we found that the chimeric protein PEBP2/CBF $\beta$ -MYH11 generated as a result of the inversion 16 and a modified form of the  $\beta$  protein was translocated into the nucleus without artificially truncating the  $\alpha$  protein. It will be interesting to examine whether this phenomenon is one of the bases for the leukemogenic potential of PEBP2/CBF $\beta$ -MYH11.

We identified two regions in  $\alpha$ A1 which harbor the elements influencing the nuclear accumulation of the protein. One is within the Runt domain and the other is in the C-terminal

region. The Runt domain was dissected into two, and each half was tested individually, but the element was not found to be exclusively localized to either half, suggesting that the signal is located in both the N- and the C-terminal halves of the Runt domain. It is not presently clear which amino acid residues are involved in the activity or how large the element is. We must also consider the possibility that the responsible amino acid residues are spread over a large area within the Runt domain. In any event, the element in the Runt domain is different from the classical nuclear localization signal composed of a cluster of several basic amino acids (14), since there is no such cluster within the Runt domain. The other element located in the C-terminal region is also devoid of a cluster of basic amino acid residues. In this case, too, the responsible elements appear to

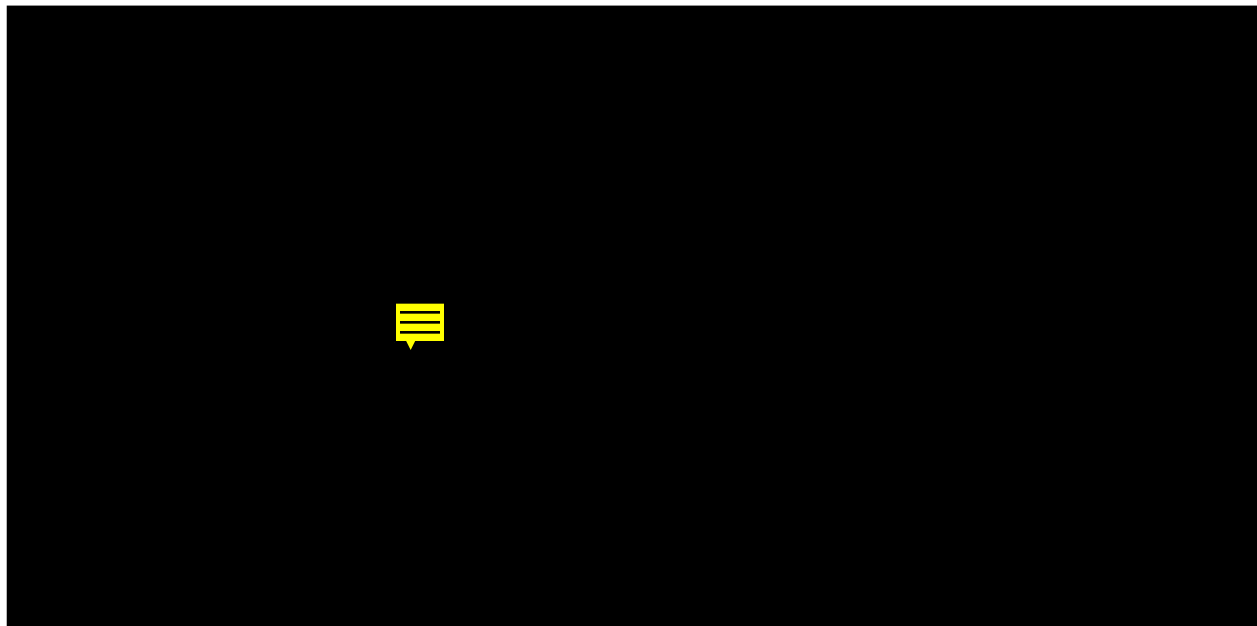


FIG. 11. Fluorescence labeling of NIH 3T3 cells transfected with the expression plasmids for PEBP2/CBF $\beta$ -MYH11 and  $\alpha$ A1. (a) Fluorescence pattern of PEBP2/CBF $\beta$ -MYH11 expressed alone and labeled with hamster anti- $\beta$ 2; (b and c) double fluorescence labeling of cells expressing PEBP2/CBF $\beta$ -MYH11 and  $\alpha$ A1 labeled by rabbit anti- $\alpha$ A1N35 and hamster anti- $\beta$ 2; (a and c) detection of rhodamine-conjugated antibody against hamster IgG with a 555-nm-wavelength filter; (b) detection of FITC-conjugated antibody against rabbit IgG with a 495-nm-wavelength filter.

be spread over a large area within the region from aa 226 to 508. It is necessary to characterize these two regions further to understand why and how such large areas are involved for this function and what the relationship between the two regions is.

The region downstream of the Runt domain of  $\alpha$ A1 and  $\alpha$ B1 is responsible for transcription activation (2, 34). Therefore, this region of the  $\alpha$  protein appears to have multiple functions: regulation of the  $\alpha/\beta$  association, regulation of the DNA-binding affinity (2), a part of the nuclear translocation activity, and transcription activation (2). In addition, this region is quite unstable. Exactly how these functions are coordinated together poses the next imperative question to be answered in exploring the mechanism and significance of the PEBP2-mediated transcriptional regulation. Of particular interest in this regard is that this important region is missing in the chimeric proteins AML1/MTG8 (ETO) and AML1/EVI1, generated as a result of t(8;21) and t(3;21) chromosome translocations, respectively. Suppositions about how the removal of this region from the AML1 protein affects its leukemogenic potential will have to await further studies.

#### ACKNOWLEDGMENTS

We thank R. Matsuoka for her generous gift of the MYH11 cDNA, N. Sawada and M. Maeda for their technical help, and M. Ueda, T. Hirama, and K. Ito for their advice on antibody techniques.

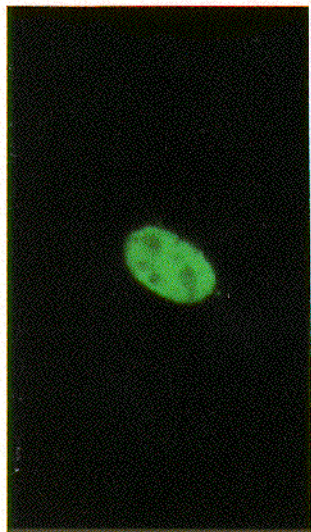
J.L. was partly supported by the Sasakawa Health Science Foundation, Japan. This work was partly supported by a grant-in-aid for Special Project Research on Cancer Bio-Science from the Ministry of Education, Science and Culture, Japan, to Y.I. (subject no. 02262215).

#### REFERENCES

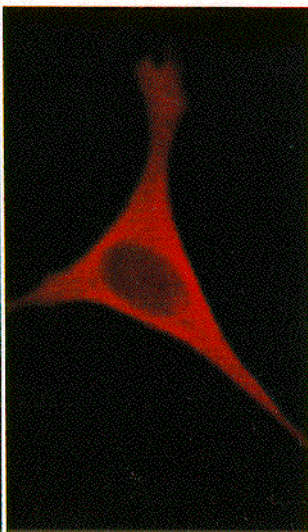
- Asano, M., Y. Murakami, K. Furukawa, Y. Yamaguchi-Iwai, M. Satake, and Y. Ito. 1990. A polyomavirus enhancer-binding protein, PEBP5, responsive to 12-*O*-tetradecanoylphorbol-13-acetate but distinct from AP-1. *J. Virol.* **64**:5927-5938.
- Bae, S. C., E. Ogawa, M. Maruyama, H. Oka, M. Satake, K. Shigesada, N. A. Jenkins, D. J. Gilbert, N. G. Copeland, and Y. Ito. 1994. PEBP2 $\alpha$ B/mouse AML1 consists of multiple isoforms that possess differential transactivation potentials. *Mol. Cell. Biol.* **14**:3242-3252.
- Bae, S. C., E. Takahashi, Y. W. Zhang, E. Ogawa, K. Shigesada, Y. Namba, M. Satake, and Y. Ito. Cloning, mapping and expression of PEBP2 $\alpha$ C, a third gene encoding the mammalian Runt domain. *Gene*, in press.
- Bae, S. C., Y. Yamaguchi-Iwai, E. Ogawa, M. Maruyama, M. Inuzuka, H. Kagoshima, K. Shigesada, M. Satake, and Y. Ito. 1993. Isolation of PEBP2 $\alpha$ B cDNA representing the mouse homolog of human acute myeloid leukemia gene, AML1. *Oncogene* **8**:809-814.
- Baeuerle, P. A., and D. Baltimore. 1988. Activation of DNA-binding activity in an apparently cytoplasmic precursor of the NF- $\kappa$ B transcription factor. *Cell* **53**:211-217.
- Chen, C., and H. Okayama. 1987. High-efficiency transformation of mammalian cells by plasmid DNA. *Mol. Cell. Biol.* **7**:2745-2752.
- Dignam, J. D., R. M. Lebovitz, and R. G. Roeder. 1983. Accurate transcription initiation by RNA polymerase II in a soluble extract from isolated mammalian nuclei. *Nucleic Acids Res.* **11**:1475-1489.
- Erickson, P., J. Gao, K.-S. Chang, T. Look, E. Whisenant, S. Raimondi, R. Lasher, J. Trujillo, J. Rowley, and H. Drabkin. 1992. Identification of break-points in t(8;21) acute myelogenous leukemia and isolation of a fusion transcript, AML1/ETO, with similarity to *Drosophila* segmentation gene *runt*. *Blood* **80**:1825-1831.
- Flanagan, W. M., B. Corthésy, R. J. Bram, and G. R. Crabtree. 1991. Nuclear association of a T-cell transcription factor blocked by FK-506 and cyclosporin A. *Nature (London)* **352**:803-807.
- Fujimura, F. K., P. L. Deininger, L. T. Friedman, and E. Linney. 1981. Mutation near the polyoma DNA replication origin permits productive infection of F9 embryonal carcinoma cells. *Cell* **23**:809-814.
- Harada, H., T. Fujita, M. Miyamoto, Y. Kimura, M. Maruyama, A. Furia, T. Miyata, and T. Taniguchi. 1989. Structurally similar but functionally distinct factors, IRF-1 and IRF-2, bind to the same regulatory elements of IFN and IFN-inducible genes. *Cell* **58**:729-739.
- Heike, T., S. Miyatake, M. Yoshida, K. Arai, and N. Arai. 1989. Bovine papilloma virus encoded E2 protein activates lymphokine genes through DNA elements, distinct from the consensus motif, in the long control region of its own genome. *EMBO J.* **8**:1411-1417.
- Kagoshima, H., K. Shigesada, M. Satake, Y. Ito, H. Miyoshi, M. Ohki, M. Pepling, and P. Gergen. 1993. The Runt domain identifies a new family of heteromeric transcriptional regulators. *Trends Genet.* **9**:338-341.
- Kalderon, D., B. L. Roberts, W. D. Richardson, and A. E. Smith. 1984. A short amino acid sequence able to specify nuclear location. *Cell* **39**:499-509.
- Kamachi, Y., E. Ogawa, M. Asano, S. Ishida, Y. Murakami, M. Satake, Y. Ito, and K. Shigesada. 1990. Purification of a mouse nuclear factor that binds to both the A and B cores of the polyomavirus enhancer. *J. Virol.* **64**:4808-4819.
- Kanda, T., K. Segawa, N. Ohuchi, S. Mori, and Y. Ito. 1994. Stimulation of

- polyomavirus DNA replication by wild-type p53 through the DNA-binding site. *Mol. Cell. Biol.* **14**:2651–2663.
17. **Kania, M. A., A. S. Bonner, J. B. Duffy, and J. P. Gergen.** 1990. The *Drosophila* segmentation gene *runt* encodes a novel nuclear regulatory protein that is also expressed in the developing nervous system. *Genes Dev.* **4**:1701–1713.
  18. **Katinka, M., M. Yaniv, M. Vasseur, and D. Blangy.** 1980. Expression of polyoma early functions in mouse embryonal carcinoma cells depends on sequence rearrangements in the beginning of the late region. *Cell* **20**:393–399.
  19. **Kozu, T., H. Miyoshi, K. Shimizu, N. Maseki, Y. Kaneko, H. Asou, N. Kamada, and M. Ohki.** 1993. Junctions of the AML1/MTG8(ETO) fusion are constant in t(8;21) acute myeloid leukemia detected by reverse transcription polymerase chain reaction. *Blood* **82**:1270–1276.
  20. **Kryszke, M. H., J. Piette, and M. Yaniv.** 1987. Induction of a factor that binds to the polyomavirus A enhancer on differentiation of embryonal carcinoma cells. *Nature (London)* **328**:254–256.
  21. **Laemmli, U. K.** 1970. Cleavage of structural proteins during the assembly of the head of bacteriophage T4. *Nature (London)* **227**:680–685.
  22. **Liu, P., S. A. Tarle, A. Hajra, D. F. Claxton, P. Marlton, M. Freedman, M. J. Siciliano, and F. S. Collins.** 1993. Fusion between transcription factor CBF $\beta$ /PEBP2 $\beta$  and a myosin heavy chain in acute myeloid leukemia. *Science* **261**:1041–1044.
  23. **Matsuoka, R., C. M. Yoshida, Y. Furutani, S. Imamura, N. Kanda, M. Yanagisawa, Y. Masaki, and A. Tkao.** 1993. Human smooth muscle myosin heavy chain gene mapped to chromosomal region 16q12. *Am. J. Med. Genet.* **46**:61–67.
  24. **Michael, A. I., H. F. David, J. S. John, and J. W. Thomas.** 1990. PCR protocol: a guide to methods and applications. Academic Press, Inc., San Diego, Calif.
  25. **Mitani, K., S. Ogawa, T. Tanaka, H. Miyoshi, M. Kurokawa, H. Mano, Y. Yazaki, M. Ohki, and H. Hirai.** 1994. Generation of the AML1-EVI-1 fusion gene in the t(3;21)(q26;q22) causes blastic crisis in chronic myeloid leukemia. *EMBO J.* **13**:504–510.
  26. **Miyatake, S., J. Shlomai, K. Arai, and N. Arai.** 1991. Characterization of the mouse granulocyte-macrophage colony-stimulating factor (GM-CSF) gene promoter: nuclear factors that interact with an element shared by three lymphokine genes—those for GM-CSF, interleukin-4 (IL-4), and IL-5. *Mol. Cell. Biol.* **11**:5894–5901.
  27. **Miyoshi, H., T. Kozu, K. Shimizu, K. Enomoto, N. Maseki, Y. Kaneko, N. Kamada, and M. Ohki.** 1993. The t(8;21) translocation in acute myeloid leukemia results in production of an AML1-MTG8(ETO) fusion transcript. *EMBO J.* **12**:2715–2721.
  28. **Miyoshi, H., K. Shimizu, T. Kozu, N. Maseki, Y. Kaneko, and M. Ohki.** 1991. t(8;21) breakpoints on chromosome 21 in acute myeloid leukemia are clustered within a limited region of a single gene, *AML1*. *Proc. Natl. Acad. Sci. USA* **88**:10431–10434.
  29. **Mizushima, S., and S. Nagata.** 1990. pEF-BOS, a powerful mammalian expression vector. 1990. pEF-BOS, a powerful mammalian expression vector. *Nucleic Acids Res.* **18**:5322.
  30. **Nisson, P. E., P. C. Watkins, and N. Sacchi.** 1992. Transcriptionally active chimeric gene derived from the fusion of the *AML1* gene and a novel gene on chromosome 8 in t(8;21) leukemic cells. *Cancer Genet. Cytogenet.* **63**:81–88.
  31. **Northrop, J. P., S. N. Ho, L. Chen, D. J. Thomas, L. A. Timmerman, G. P. Nolan, A. Admon, and G. R. Crabtree.** 1994. NF-AT components define a family of transcription factors targeted in T-cell activation. *Nature (London)* **369**:497–502.
  32. **Nucifora, G., D. J. Birn, P. Erickson, J. Gao, M. M. LeBeau, H. A. Drabkin, and J. D. Rowley.** 1993. Detection of DNA rearrangements in the AML1 and ETO loci and of an AML1/ETO fusion mRNA in patients with t(8;21) acute myeloid leukemia. *Blood* **81**:883–888.
  33. **Ogawa, E., M. Inuzuka, M. Maruyama, M. Satake, M. Naito-Fujimoto, Y. Ito, and K. Shigesada.** 1993. Molecular cloning and characterization of PEBP2 $\beta$ , the heterodimeric partner of a novel *Drosophila runt*-related DNA binding protein PEBP2 $\alpha$ . *Virology* **194**:314–331.
  34. **Ogawa, E., and Y. Ito.** Unpublished data.
  35. **Ogawa, E., M. Maruyama, H. Kagoshima, M. Inuzuka, J. Lu, M. Satake, K. Shigesada, and Y. Ito.** 1993. PEBP2/PEA2 represents a family of transcription factors homologous to the products of the *Drosophila runt* gene and the human AML1 gene. *Proc. Natl. Acad. Sci. USA* **90**:6859–6863.
  36. **Pagano, M., M. Dürst, S. Joswig, G. Draetta, and P. Jansen-Dürr.** 1992. Binding of the human E2F transcription factor to the retinoblastoma protein but not to cyclin A is abolished in HPV-16-immortalized cells. *Oncogene* **7**:1681–1686.
  37. **Piette, J., and M. Yaniv.** 1987. Two different factors bind to the  $\alpha$ -domain of the polyoma virus enhancer, one of which also interacts with the SV40 and c-fos enhancers. *EMBO J.* **6**:1331–1337.
  38. **Rogers, S., R. Wells, and M. Rechsteiner.** 1986. Amino acid sequences common to rapidly degraded proteins: the PEST hypothesis. *Science* **234**:364–368.
  39. **Rosenberg, A. H., B. N. Lade, D.-S. Chui, S. W. Lin, J. J. Dunn, and F. W. Studier.** 1987. Vectors for selective expression of cloned DNAs by T7 RNA polymerase. *Gene* **56**:125–135.
  40. **Sakakura, C., Y. Yamaguchi-Iwai, M. Satake, S. C. Bae, A. Takahashi, E. Ogawa, A. Hagiwara, T. Takahashi, A. Murakami, K. Makino, T. Nakagawa, N. Kamada, and Y. Ito.** 1994. Growth inhibition and induction of differentiation of t(8;21) acute myeloid leukemia cells by the DNA binding domain of PEBP2 and the AML1/MTG8(ETO) specific antisense oligonucleotide. *Proc. Natl. Acad. Sci. USA* **91**:11723–11727.
  41. **Sambrook, J., E. F. Fritsch, and T. Maniatis.** 1989. Molecular cloning: a laboratory manual, 2nd ed. Cold Spring Harbor Laboratory Press, Cold Spring Harbor, N.Y.
  42. **Satake, M., T. Ibaraki, and Y. Ito.** 1988. Modulation of polyomavirus enhancer binding proteins by Ha-*ras* oncogene. *Oncogene* **3**:69–78.
  43. **Satake, M., S. Nomura, Y. Yamaguchi-Iwai, Y. Takahama, Y. Hashimoto, M. Niki, Y. Kitamura, and Y. Ito.** 1995. Expression of the Runt domain-encoding PEBP2 $\alpha$  genes in T cells during thymic development. *Mol. Cell. Biol.* **15**:1662–1670.
  44. **Sekikawa, K., and A. J. Levine.** 1981. Isolation and characterization of polyoma host range mutants that replicate in nullipotent embryonal carcinoma cells. *Proc. Natl. Acad. Sci. USA* **78**:1100–1104.
  45. **Studier, F. W., and B. A. Moffatt.** 1986. Use of bacteriophage T7 RNA polymerase to direct selective high-level expression of cloned genes. *J. Mol. Biol.* **189**:113–130.
  46. **Wang, S., Q. Wang, B. E. Crute, I. N. Melnikova, S. R. Keller, and N. A. Speck.** 1993. Cloning and characterization of subunits of the T-cell receptor and murine leukemia virus enhancer core-binding factor. *Mol. Cell. Biol.* **13**:3324–3339.

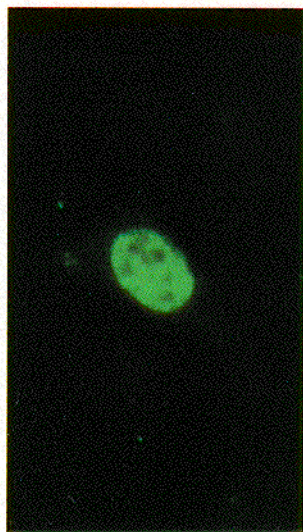
(a)



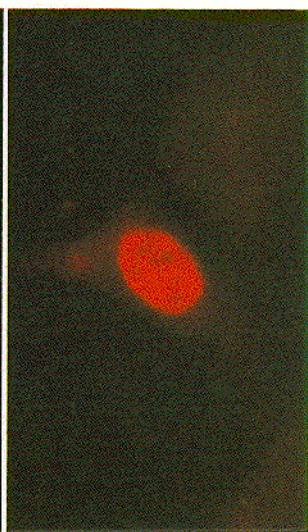
(b)



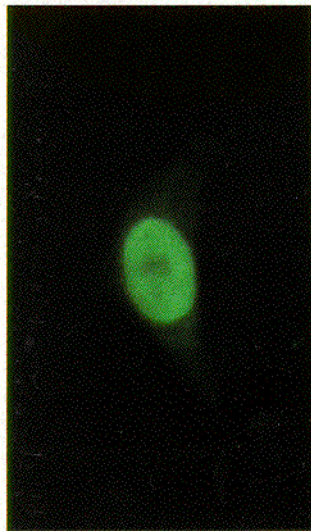
(c)



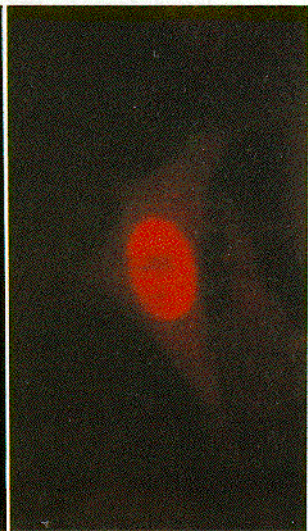
(d)



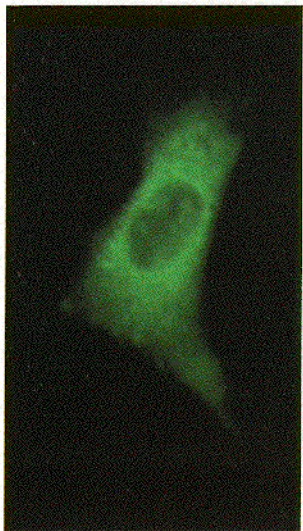
(e)



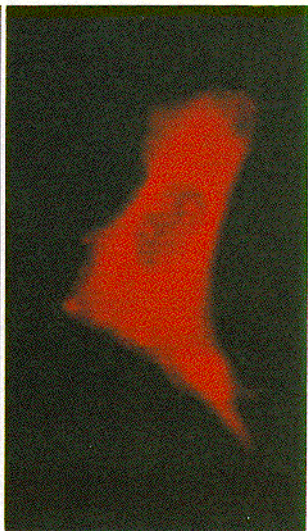
(f)



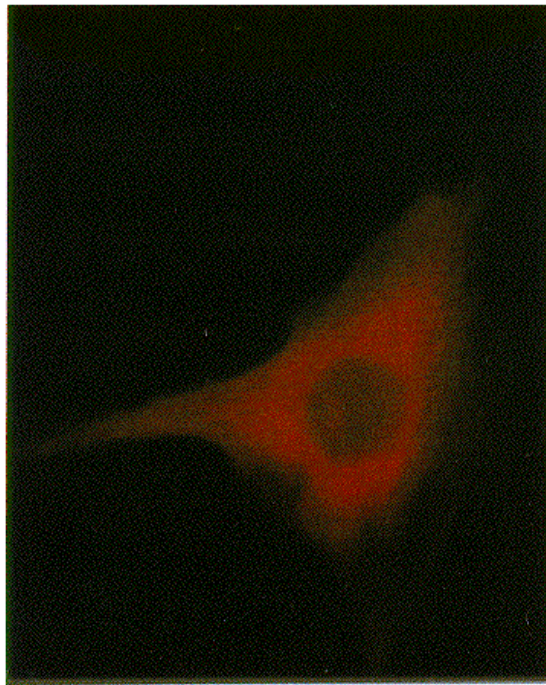
(g)



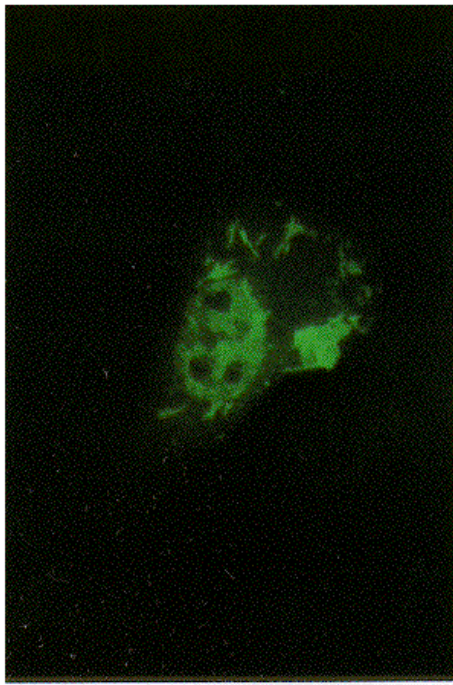
(h)



a



b



c

